J. Fluid Mech. (2003), *vol.* 495, *pp.* 145–156.
DOI: 10.1017/S0022112003006037 Printed in the United Kingdom

Standing waves on water of uniform depth: on their resonances and matching with short-crested waves

By M. OKAMURA[1], M. IOUALALEN[2] AND C. KHARIF[3]

[1]Research Institute for Applied Mechanics, Kyushu University, Kasuga, Fukuoka 816-8580, Japan

[2]Institut de Recherche pour le Développement, BP A5, 98848 Nouméa Cedex, New-Caledonia

[3]Institut de Recherche sur les Phénomènes Hors Equilibre, 49, rue F. Joliot-Curie, BP 146, F13384, Marseille Cedex 13, France

(Received 10 May 2003 and in revised form 11 July 2003)

Numerical calculations of the resonant interactions of three-dimensional short-crested waves very near their two-dimensional standing wave limit are performed for water of uniform depth. A detailed study of the properties of the solutions indicates that both classes of waves admit multiple solutions that are connected to each other through turning points. It is also shown that the solutions match each other at the limit. Then a study on the superharmonic instabilities (resonant interactions) of short-crested waves was performed in the vicinity of the standing wave limit. The matching allowed extrapolation of the short-crested wave stability results to standing waves. The results are that for resonant waves, superharmonic instabilities associated with harmonic resonance are dominant. The possible jumps from one solution to another may lead to a drastic change of the wave itself. Since the superharmonic instability enhances this property one may conclude that this class of waves can be considered non-stationary. By contrast, non-resonant waves are weakly unstable or stable and are the only waves that are likely to exist. Thus, this class of waves can be considered as quasi-permanent.

1. Introduction

Two-dimensional standing waves may be described as confined waves that are subject to two boundary conditions at their extremities. Mercer & Roberts (1994) showed that the strongest (lowest order) harmonic resonance appears at the fifth order of the solution. The linear theory associates the harmonic resonance with non-uniqueness of the solutions. Standing waves represent one limit of three-dimensional short-crested wave fields. These latter waves are defined as a superposition of two two-dimensional progressive wave trains of equal wavelengths intersecting at angle γ. A description of short-crested waves can be found in Hsu, Tsuchiya & Silvester (1979) who defined the angle θ as $\theta = (\pi - \gamma)/2$. Based on a variational approach, Bridges, Dias & Menasce (2001) provided a new formulation of the problem of steady doubly periodic patterns on finite-depth fluid including a uniform mean flow. The standing wave limit corresponds to angle $\theta = 0^\circ$, i.e. two progressive waves propagate in opposite directions. The other two-dimensional limit is the progressive Stokes wave for $\theta = 90^\circ$, i.e. the two waves propagate in the same direction.

Roberts (1983) and Marchant & Roberts (1987) discussed the properties of short-crested waves for deep water and water of finite depth respectively. In particular, they showed how short-crested wave fields may be unsteady through harmonic resonance phenomena. Later, Ioualalen, Roberts & Kharif (1996) and Ioualalen, Kharif & Roberts (1999) showed for finite depth water that a harmonic resonance of an asymptotic short-crested wave solution is associated with a sporadic and weak superharmonic instability that is not likely to develop. In particular, the associated instability exhibits a bubble-like shape in the wave steepness parameter space. Their short-crested wave solutions were not complete however because they computed and analysed only one branch of the solution associated with harmonic resonance. Later, for a single (one only) harmonic resonance, Ioualalen & Okamura (2002) computed fully nonlinear short-crested waves with their characteristic multiple solution, i.e. two branches matching each other through a turning point plus one single branch. They found that the solutions computed by Ioualalen *et al.* (1996, 1999) were incomplete when a harmonic resonance occurs because they do not take into account the bifurcation process between the different branches. They also computed the stability diagram in the vicinity of a harmonic resonance and found that a single harmonic resonance is associated with two bubbles of instability that are no longer sporadic.

Very little work has been done near the two-dimensional limits of short-crested waves, i.e. on how short-crested wave fields match standing waves. Okamura (1996) showed that short-crested waves match standing waves in deep water for $\theta \to 0^\circ$. However the question still remains for standing waves on finite depth. Marchant & Roberts (1987) and Mercer & Roberts (1994) showed that harmonic resonances occur for standing waves on finite depth if a harmonic (m, n), that is, $\sin(m\omega t)\cos(ny)\cosh[n(z+d)]$, is solution of the homogeneous differential equation derived from the nonlinear surface conditions of the standing wave. Such a case occurs at critical depths for which

$$n \tanh(nd) = m^2 \tanh d. \tag{1.1}$$

Marchant & Roberts (1987) calculated the critical depths for which a harmonic resonance occurs. The lowest-order harmonic resonance (3, 5), is generated at depth $d_{hr} \approx 0.624$.

In the present study, the matching between approximate short-crested waves and standing waves is analysed near that critical depth. Note that all solutions discussed in the paper are approximated because of the presence of the harmonic resonances. Then a superharmonic stability analysis is performed in order to examine the time scales of the harmonic resonances for short-crested waves very near the standing wave limit, i.e for $\theta \to 0^\circ$. This is because our stability numerical procedure does not apply directly to non-stationary standing waves.

2. General equations and numerical procedures

We consider surface gravity waves on an inviscid incompressible fluid of finite depth where the flow is assumed irrotational. The governing equations are given in a dimensionless form with respect to the reference length $1/k$ and the reference time $(gk)^{-1/2}$, where g is the gravitational acceleration and k the wavenumber of the incident wave train.

Let us define a frame of reference $(x^*, y^*, z^*, t^*, \phi^*)$ so that $x^* = x - ct$, $y^* = y$, $z^* = z$, $t^* = t$ and $\phi^* = \phi - cx^*$ where c represents the propagation velocity of the short-crested wave train and is equal to ω/α, ω being the frequency of the wave and

$\alpha = \sin\theta$ is the x-direction wavenumber, the y-direction wavenumber being $\beta = \cos\theta$. If we omit the asterisks for simplicity, the governing equations are

$$\Delta\phi = 0 \quad \text{for } -d < z < \eta, \tag{2.1}$$

$$\phi_z = 0 \quad \text{on } z = -d, \tag{2.2}$$

$$\phi_t + \eta + \tfrac{1}{2}\left(\phi_x^2 + \phi_y^2 + \phi_z^2 - c^2\right) = 0 \quad \text{on } z = \eta, \tag{2.3}$$

$$\eta_t + \phi_x\eta_x + \phi_y\eta_y - \phi_z = 0 \quad \text{on } z = \eta, \tag{2.4}$$

where d is the depth of the fluid, $\phi(x, y, z, t)$ is the velocity potential and $z = \eta(x, y, t)$ is the equation of the free surface. In this new frame of reference propagating at a speed c, the system of equations (2.1)–(2.4) admits doubly periodic solutions of permanent form $\bar{\eta}(x, y)$ and $\bar{\phi}(x, y, z)$.

Like Ioualalen *et al.* (1999), we define the following functions to construct a stability problem:

$$\eta(x, y, t) = \bar{\eta}(x, y) + \eta'(x, y, t), \tag{2.5}$$

$$\phi(x, y, z, t) = \bar{\phi}(x, y, z) + \phi'(x, y, z, t), \tag{2.6}$$

where we assume that the surface elevation and the velocity potential are the superposition of a steady unperturbed wave $(\bar{\eta}, \bar{\phi})$ and infinitesimal unsteady perturbations (η', ϕ') where $\eta' \ll \bar{\eta}$ and $\phi' \ll \bar{\phi}$. After substituting (2.5) and (2.6) into equations (2.1)–(2.4) and linearizing, we obtain the zeroth-order system of equations for which permanent short-crested waves are solutions and then the first-order perturbation equations representing the stability problem. Both systems of equations will be solved in the frame of reference moving with the wave.

The zeroth-order system of equations is as follows:

$$\Delta\bar{\phi} = 0 \quad \text{for } -d < z < \bar{\eta}, \tag{2.7}$$

$$\bar{\phi}_z = 0 \quad \text{on } z = -d, \tag{2.8}$$

$$\bar{\eta} + \tfrac{1}{2}\left(\bar{\phi}_x^2 + \bar{\phi}_y^2 + \bar{\phi}_z^2 - c^2\right) = 0 \quad \text{on } z = \bar{\eta}, \tag{2.9}$$

$$\bar{\phi}_x\bar{\eta}_x + \bar{\phi}_y\bar{\eta}_y - \bar{\phi}_z = 0 \quad \text{on } z = \bar{\eta}. \tag{2.10}$$

The wave steepness is defined as

$$h = \frac{\bar{\eta}(0, 0) - \bar{\eta}(\pi/\alpha, 0)}{2}, \tag{2.11}$$

which is the half of the non-dimensional peak-to-trough height for non-resonant waves. The numerical method to obtain short-crested wave solutions of permanent form is described in Okamura (1996) and Ioualalen & Okamura (2002). We look for the following form of the velocity potential:

$$\bar{\phi} = -cx + \sum_{k=0}^{N} \sum_{j=2-(k \bmod 2)}^{N} \phi_{j,k} \sin(j\alpha x)\cos(k\beta y)\frac{\cosh[\kappa_{j,k}(z + d)]}{\cosh(\kappa_{j,k}d)}, \tag{2.12}$$

where $\kappa_{j,k} = [(j\alpha)^2 + (k\beta)^2]^{1/2}$ and N is the maximum order of expansion and is chosen to be odd. All calculations are carried out by increasing N until convergence. Further details about the computations of the short-crested waves can be found in Okamura (1996).

Note that at the limit $(\theta \to 0^\circ, \alpha \to 0)$, we obtain $\phi_{j,k}\sin(j\alpha x^*) = \phi_{j,k}\sin[j\alpha(x - ct)] = -\phi_{j,k}\sin(j\omega t)$, with $c = \omega/\alpha$. In that case, we look for solutions independently,

without reference to angle θ to avoid any artificial computational overflow of the term ω/α when $\alpha = 0$.

Then the first-order system of equations is

$$\Delta\phi' = 0 \quad \text{for } -d < z < \bar{\eta}, \tag{2.13}$$

$$\phi'_z = 0 \quad \text{on } z = -d, \tag{2.14}$$

$$\phi'_t = -\bar{\phi}_x\phi'_x - \bar{\phi}_y\phi'_y - \bar{\phi}_z\phi'_z - \eta'(1 + \bar{\phi}_x\bar{\phi}_{xz} + \bar{\phi}_y\bar{\phi}_{yz} + \bar{\phi}_z\bar{\phi}_{zz}) \quad \text{on } z = \bar{\eta}, \tag{2.15}$$

$$\eta'_t = \eta'(\bar{\phi}_{zz} - \bar{\eta}_x\bar{\phi}_{xz} - \bar{\eta}_y\bar{\phi}_{yz}) - \bar{\eta}_x\phi'_x - \bar{\phi}_x\eta'_x - \bar{\eta}_y\phi'_y - \bar{\phi}_y\eta'_y + \phi'_z \quad \text{on } z = \bar{\eta}, \tag{2.16}$$

for which we look for non-trivial solutions of the following form:

$$\eta' = \mathrm{e}^{-\mathrm{i}\sigma t} \sum_{J=-\infty}^{\infty} \sum_{K=-\infty}^{\infty} a_{J,K} \mathrm{e}^{\mathrm{i}(J\alpha x + K\beta y)}, \tag{2.17}$$

$$\phi' = \mathrm{e}^{-\mathrm{i}\sigma t} \sum_{J=-\infty}^{\infty} \sum_{K=-\infty}^{\infty} b_{J,K} \mathrm{e}^{\mathrm{i}(J\alpha x + K\beta y)} \frac{\cosh[\kappa_{J,K}(z+d)]}{\cosh(\kappa_{J,K} d)}. \tag{2.18}$$

The resolution of this eigenvalue problem consists of a stability analysis for which we need to determine the set of eigenvalues σ and the coefficients $a_{J,K}$ and $b_{J,K}$ of their associated eigenvectors. Since the system of equations (2.13)–(2.16) represents a Hamiltonian structure, the eigenvalues σ appear in complex-conjugate pairs. Thus an instability corresponds to $\mathrm{Im}(\sigma) \neq 0$. For wave steepness $h = 0$, the unperturbed wave is given by $\bar{\eta} = 0$ and $\bar{\phi} = -c_0 x$ with $c_0 = \omega_0/\alpha = (\tanh d)^{1/2}/\alpha$. Then the eigenvalues are

$$\sigma^s_{J,K} = -J\alpha c_0 + s[\kappa_{J,K} \tanh(\kappa_{J,K} d)]^{1/2}, \qquad s = \pm 1, \tag{2.19}$$

where the signature of the perturbation is defined as $\mathrm{sign}[s\mathrm{Im}(-\mathrm{i}\sigma)]$, e.g. MacKay & Saffman (1986). The set of eigenvalues $\{\sigma^s_{J,K}\}$ is neutrally stable for $h = 0$. Instabilities arise as the wave steepness h increases. We use here the approach of Ioualalen *et al.* (1999), which takes advantage of the useful work of MacKay & Saffman (1986) on Hamiltonian systems. We apply the necessary condition for instability in terms of eigenvalue collisions of opposite signatures or at zero frequency: given a wave steepness h, an instability can arise if two modes have the same frequency, that is, $\sigma^s_{J_1,K_1} = \sigma^{-s}_{J_2,K_2}$. This condition takes the following form for $s = 1$ ($s = -1$ corresponds to an opposite direction of propagation):

$$\left[\kappa_{J_1,K_1} \tanh\left(\kappa_{J_1,K_1} d\right)\right]^{1/2} + \left[\kappa_{J_2,K_2} \tanh\left(\kappa_{J_2,K_2} d\right)\right]^{1/2} = (J_1 - J_2) \tanh^{1/2} d. \tag{2.20}$$

The numerical procedure to solve the eigenvalue problem is detailed in Ioualalen & Okamura (2002).

3. Standing and short-crested waves: their characteristics and matching

The resonance condition (1.1) shows that standing waves in deep water do not encounter harmonic resonances while standing waves on water of finite depth are subject to them. We analyse in this section the fifth-order (3, 5) resonance which occurs at depth $d_{hr} \approx 0.624$ because it is the strongest harmonic resonance. We will consider the following two configurations.

In the first case, we will consider only the single (3, 5) harmonic resonance without reference to any other resonance that may occur around the critical depth $d_{hr} \approx 0.624$. It will be shown that single resonances may yield three distinct branch solutions within

Order N	$\phi_{1,1}=0.06,\ d=0.62$	$\phi_{1,1}=0.2,\ d=0.58$
	branch $(1)_{3,5}$	
17	$-1.865310696\times10^{-5}$	$-3.951763321\times10^{-4}$
19	$-1.865310696\times10^{-5}$	$-3.951769609\times10^{-4}$
21	$-1.865310696\times10^{-5}$	$-3.951769684\times10^{-4}$
23		$-3.951769603\times10^{-4}$
25		$-3.951769654\times10^{-4}$
27		$-3.951769654\times10^{-4}$
	branch $(2)_{3,5}$	
17	$-5.746762898\times10^{-3}$	
19	$-5.746764507\times10^{-3}$	$-1.472865889\times10^{-2}$
21	$-5.746772968\times10^{-3}$	$-1.468852549\times10^{-2}$
23	$-5.746765198\times10^{-3}$	$-1.469538390\times10^{-2}$
25	$-5.746765216\times10^{-3}$	$-1.468928159\times10^{-2}$
27	$-5.746765226\times10^{-3}$	$-1.468747941\times10^{-2}$
29	$-5.746765227\times10^{-3}$	$-1.468570117\times10^{-2}$
31		$-1.468223799\times10^{-2}$
33		$-1.468544388\times10^{-2}$
35		$-1.468572651\times10^{-2}$
37		$-1.468585037\times10^{-2}$
	branch $(3)_{3,5}$	
17	5.756929317×10^{-3}	
19	5.756929150×10^{-3}	1.411678337×10^{-2}
21	5.756931649×10^{-3}	1.414900982×10^{-2}
23	5.756929623×10^{-3}	1.416705818×10^{-2}
25	5.756929550×10^{-3}	1.421423636×10^{-2}
27	5.756929542×10^{-3}	1.422469017×10^{-2}
29	5.756929542×10^{-3}	1.421178330×10^{-2}
31		1.420996969×10^{-2}
33		1.420585906×10^{-2}
35		1.420308851×10^{-2}
37		1.420163614×10^{-2}

TABLE 1. Values of $\phi_{3,5}$ at angle $\theta=0.001^\circ$ for $\phi_{1,1}=0.06$, $d=0.62$ and $\phi_{1,1}=0.2$, $d=0.58$, as a function of the order N of truncation.

a certain range of the wave steepness. Since the d-nearest harmonic resonance occurs at the 20th-order (for critical depth depth $d_{hr}\approx0.627$), the solutions will be computed at order $N=19$ (the order immediately lower than the order of appearence), for which they numerically converge.

In the second case, we will also consider the $(6, 20)$ higher-order resonance that is due to the nearest other critical depth $d_{hr}\approx0.627$ (Ioualalen *et al.* 1996). That particular case is a first step in the analysis of the behaviour of short-crested waves in the presence of multiple harmonic resonances; the solutions may have at most 3^M branches, where M is the number of harmonic resonances. The solutions will be computed for $N>20$.

In order to illustrate the effects of high-order resonances, we provide in table 1 an example of the convergence of $\phi_{3,5}$ for two configurations. For weak $\phi_{1,1}$ ($\phi_{1,1}=0.06$, $d=0.62$), the branch solution $(1)_{3,5}$ has converged at order $N=17$ ($N<20$). The convergence of the two other branches is particular: we first observe a reasonable convergence from $N=17$ to $N=19$, then it deteriorates from $N=19$ to $N=21$

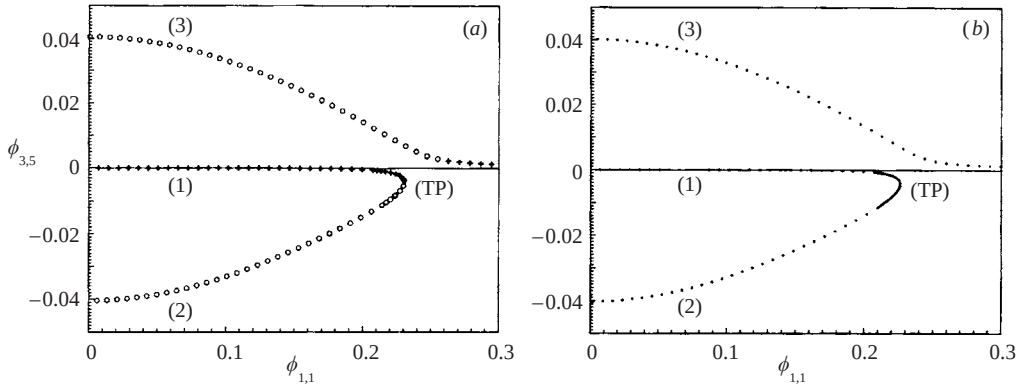

FIGURE 1. Coefficient $\phi_{3,5}$ versus coefficient $\phi_{1,1}$ for depth $d = 0.58$ and (a) $\theta = 0°$ and (b) $\theta = 5°$. The different branches of the solutions are numbered (1)–(3) and (TP) is used for a turning point. Circles denote the unstable solutions while plus-signs correspond to stable solutions (displayed only for $\theta = 0°$).

(occurrence of the (6, 20) harmonic resonance), and finally it improves with N increasing. We attribute this deterioration to the active effects of the appearance of (6, 20) resonant modes that are non-resonant for $N < 20$. The other reason is that since each $\phi_{3,5}$ branch is subject to variations when a jump of the $\phi_{6,20}$ solution occurs from one branch to another, the convergenve can be slower. In fact this aspect is not linked to the numerical convergence of the solutions but rather to their identification when branches of (6, 20) are very close. This point will be discussed later. For larger $\phi_{1,1}$ ($\phi_{1,1} = 0.2$, $d = 0.58$), we do not observe this convergence behaviour because the dominant feature is the difficulty in obtaining convergence and the necessity to increase N substantially in order to validate the solutions.

3.1. *Introduction: the single resonance case*

Figure 1 exhibits the multiple solution structure of the coefficient $\phi_{3,5}$ as a function of the coefficient $\phi_{1,1}$ of the fundamental mode for depth $d = 0.58$ and angles $\theta = 0°$ ('pure' standing wave) and $\theta = 5°$ (short-crested wave near the standing wave limit). A high-density computation has been performed in the vicinity of the turning points, $\phi_{1,1} \approx 0.2305605$ and $\phi_{1,1} \approx 0.226085$, for which bifurcations of the waves occur. The solutions are composed of three branches: branches (1) and (2) which are connected through a turning point (TP) and the single branch (3). For both angles the shape of the solution exhibits the same characteristics and their amplitudes are fairly similar. Note that the solutions on the left-hand side of the ($\phi_{1,1}$, $\phi_{3,5}$)-plane are not shown because they are symmetrical about the origin.

Figure 1 also indicates that the resonant harmonic mode $\phi_{3,5}$ can be significant both on branch (2) and on branch (3) for $\phi_{1,1}$ smaller than the turning point (TP) while it is not significant on branch (1) and branch (3) beyond the (TP), dominated by mode $\phi_{1,1}$. We call them a resonant wave and a non-resonant wave respectively. Consequently, for resonant waves near $\phi_{1,1} = 0$, it is most interesting to note that the coefficient $\phi_{3,5}$ dominates the harmonic structure. This can be interpreted as follows: in the presence of a resonant interaction, the wave is likely to undergo a superharmonic transition. Note also that the stable branches (branch (1) and part of branch (3) close to the $\phi_{1,1}$-axis) correspond to the waves that are most likely to be observed.

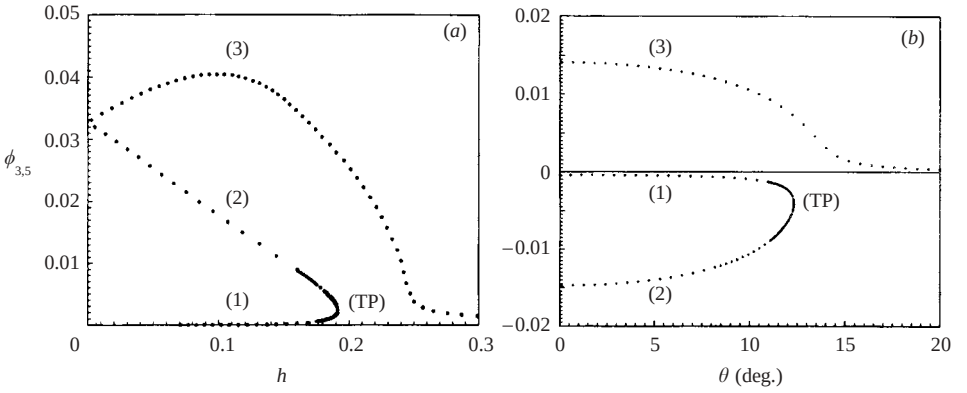

FIGURE 2. Coefficient $\phi_{3,5}$ versus (a) wave steepness h for $d = 0.58$ and $\theta = 0°$, and (b) angle θ for $d = 0.58$ and $\phi_{1,1} = 0.2$.

Figure 2(a) shows the multiple solution structure of the coefficient $\phi_{3,5}$ as a function of the wave steepness h instead of the fundamental mode $\phi_{1,1}$ (figure 1) for depth $d = 0.58$ and angle $\theta = 0°$. Note that solutions on the lower half of the $(h, \phi_{3,5})$-plane are not shown because they are symmetrical about the h-axis. The turning point in the $(h, \phi_{3,5})$-plane appears at $h \approx 0.1914786$ corresponding to $\phi_{1,1} \approx 0.22774$. That means that the place where the turning point appears in the $(h, \phi_{3,5})$-plane is different from that in the $(\phi_{1,1}, \phi_{3,5})$-plane.

In figure 2(b) we show a bifurcation diagram of the solutions as a function of angle θ for depth $d = 0.58$ and coefficient $\phi_{1,1} = 0.2$. Such harmonic resonances, exhibiting a multiple solution structure, are specific to standing waves on water of finite depth and contaminate the short-crested wave field up to angle $\theta_{cr} \approx 14.5°$. At a greater angle, i.e. a more three-dimensional wave, the short-crested wave has a unique solution. Note that this critical angle applies for these particular parameters $(d, \phi_{1,1}) = (0.58, 0.2)$. More generally (not shown here), the critical angle θ_{cr} is a function of parameters d and $\phi_{1,1}$.

Another main feature of figure 2(b) is the continuous matching between 'pure' two-dimensional standing waves and three-dimensional short-crested wave solutions. This is an important aspect of the study since we are now able to apply the stability analysis/results of short-crested wave solutions for $\theta \to 0°$ (but non-zero) to 'pure' two-dimensional standing waves. $\theta = 0.001°$ will be taken in the following.

3.2. *The multiple resonance case*

In this case we took depth $d = 0.62$ in order to compute more easily the solutions and have access to most of the solution branches. At that depth, the wave is subject to (3, 5) and (6, 20) resonances appearing at orders 5 and 20 respectively. We have computed solutions past the order of truncation 20 in order to obtain the two resonances. In figure 3 we report some of the branches of solutions $\phi_{3,5}$ and $\phi_{6,20}$. Our aim here is to exhibit the cross-effects of $\phi_{3,5}$ and $\phi_{6,20}$ branch solutions. Figure 3(a) shows the two possible solutions of branch $(3)_{3,5}$ when a jump from branch $(1)_{6,20}$ to branch $(2)_{6,20}$ occurs. The difference between the two solutions is not observable on the plot. At $\phi_{1,1} = 0.1084756$ and $\phi_{1,1} = 0.1085133$, the relative gaps between the two possible converged solutions of $(3)_{3,5}$ are 3×10^{-3} and 1.5×10^{-4} respectively. The gap is relatively weak but still the two distinct solutions (a1) and (a2) are observable in our computations. Figure 3(b) shows the two possible solutions of branch $(2)_{3,5}$ when

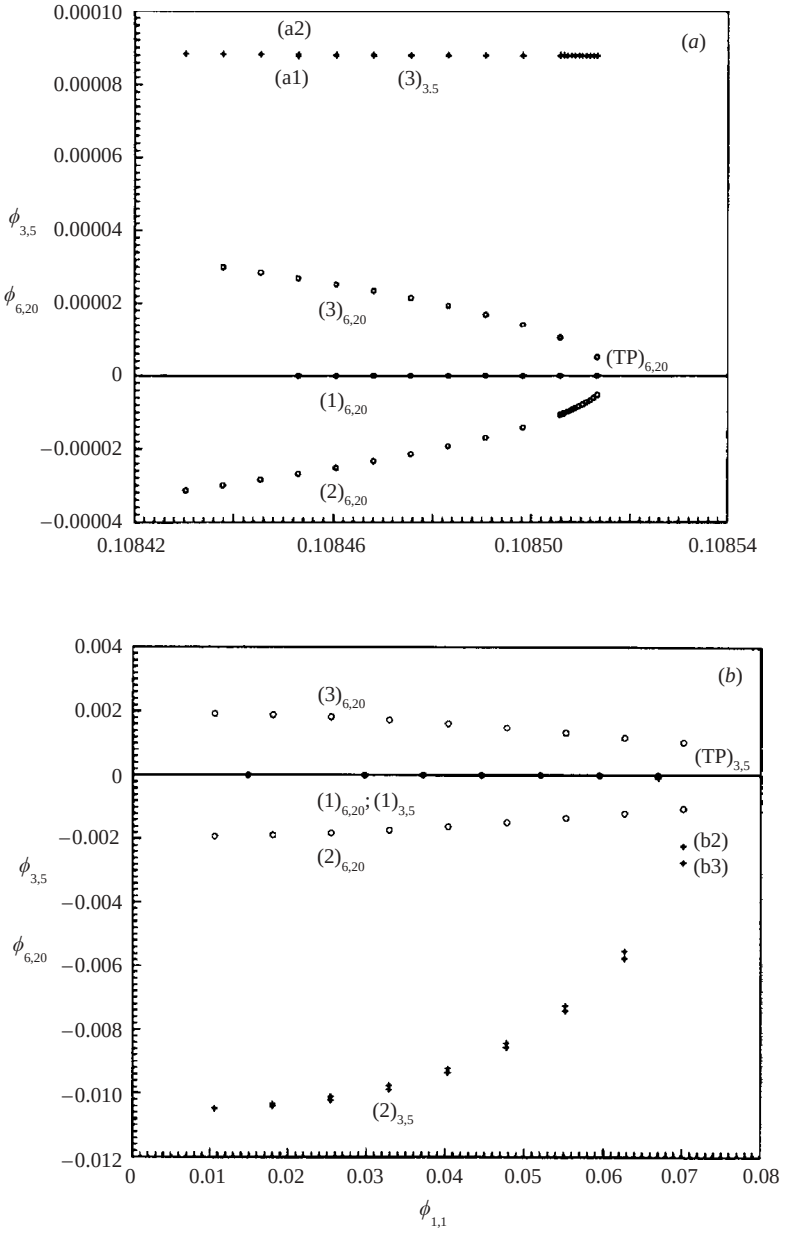

FIGURE 3. Coefficients $\phi_{3,5}$ and $\phi_{6,20}$ versus $\phi_{1,1}$ for $d = 0.62$ and $\theta = 0.001°$. (*a*) A portion of the plane where we observe the three branches and the turning point of resonance coefficient $\phi_{6,20}$, i.e. $(1)_{6,20}$, $(2)_{6,20}$, $(3)_{6,20}$ and $(TP)_{6,20}$ (circles), and branches (3) of coeffcient $\phi_{3,5}$ (plus-signs), i.e. $(3)_{3,5}$, that are computed for the distinct $(1)_{6,20}$, $(2)_{6,20}$ [(a1) and (a2) respectively]. Note that the two $(3)_{3,5}$ branches are hardly differentiable in the plot. (*b*) A portion of the parameter regime where we found successive couples of branch $(2)_{3,5}$ [(b2) and (b3)] when a jump of the solution $\phi_{6,20}$ occurs from branch $(2)_{6,20}$ to branch $(3)_{6,20}$ respectively.

a jump from branch $(2)_{6,20}$ to branch $(3)_{6,20}$ occurs. In that case the two solutions (b2) and (b3) appear clearly on the figure. At $\phi_{1,1} = 0.01060$ and $\phi_{1,1} = 0.07015$, the relative gaps between the two solutions are 3×10^{-5} and 5×10^{-4}. Here again the

converged solutions are computable. In both cases the gap between the two solutions is more important around the $\phi_{6,20}$ turning point but on the whole it is relatively weak.

4. Superharmonic instability of short-crested waves near their standing wave limit: $\theta = 0.001^\circ$

We calculate here the superharmonic instabilities of short-crested waves that are very close to standing waves; that is, $\theta = 0.001^\circ$. Since Ioualalen & Okamura (2002) clarified the relation between a superharmonic instability and a harmonic resonance for short-crested waves, we wish here to characterize the superharmonic instabilities associated with harmonic resonances of standing waves. The time scale of the strongest instability will tell us whether the multiple solution related to harmonic resonance is observable. For this stability analysis we have chosen $\phi_{3,5}$ branch solutions for the single resonance case. We made this choice because (i) the stability results will be more general, (ii) the relative gap between two solutions of one $\phi_{3,5}$ branch solution relative to two distinct $\phi_{3,5}$ branches is weak thus (iii) the derived stability results will be representative.

Following Ioualalen *et al.* (1996), a superharmonic instability associated with a harmonic resonance (m, n) can arise only if the two eigenvalues $\sigma^{s}_{m,n}(h)$ and $\sigma^{-s}_{-m,n}(h)$ merge at zero. For standing waves the condition of harmonic resonance is equivalent to the relation (1.1). The coalescence of the two eigenmodes $(\pm m, n)$ is then interpreted as Ioualalen *et al.* (1999)'s class Ia(m, n) instability. Such superharmonic instability is described as an interaction between the two eigenmodes $(\pm m, n)$ and the $2m$-modes $(1, \pm 1)$ of the basic unperturbed standing wave; that is,

$$\Omega_1 = -\Omega_2 + m\Omega_{01} + m\Omega_{02}, \tag{4.1}$$

$$k_1 = k_2 + mk_{01} + mk_{02}, \tag{4.2}$$

where $\Omega_i = [|k_i| \tanh(\kappa_{m,n} d)]^{1/2}$, $\Omega_{0i} = \tanh^{1/2} d$ for $i = 1, 2$ and $k_1 = (\alpha m, \beta n)$, $k_2 = (-\alpha m, \beta n)$, $k_{01} = (\alpha, \beta)$, and $k_{02} = (\alpha, -\beta)$.

In figures 4 and 5 the frequencies and growth rates of the eigenvalues $\sigma_{\pm 3,5}$ are plotted for all branches of the wave solutions for depths $d = 0.58$ and $d = 0.62$ in the vicinity of the critical depth $d_{hr} \approx 0.624$. For both depths, branch (1) is always stable, i.e. from $\phi_{1,1} = 0$ to the turning point ($\phi_{1,1} \approx 0.2305605$ for $d = 0.58$ and $\phi_{1,1} \approx 0.0705$ for $d = 0.62$). By contrast, branch (2) is always unstable. The transition from stability to instability occurs when the frequency reaches the zero-axis: then the growth rate value leaves the axis. For both depths, the dominant instability appears when $\phi_{3,5}$ is dominant while $\phi_{1,1}$ is negligible. Instability of branch (2) weakens with decreasing $\phi_{3,5}$ then cancels at the turning point (at the zero-axis here). A similar behaviour is observed for branch (3) except that instability disappears beyond the turning point ($\phi_{1,1} \approx 0.2591$ for $d = 0.58$ and $\phi_{1,1} \approx 0.0709$ for $d = 0.62$). The maximum instability also appears for $\phi_{1,1}$ negligible. The instability occurs when eigenvalues $\sigma_{3,5}$ and $\sigma_{-3,5}$ coalesce at zero frequency (phase-locked with the unperturbed wave). Such instability is physically associated with a resonant interaction: the coalescence of the two eigenmodes at zero frequency simply means that the harmonics $(\pm 3, 5)$ propagate at the same phase speed as the basic wave, bearing in mind that the stability problem has been computed in the frame of reference moving with the basic wave.

So far, this behaviour has not been identified. Previous studies showed that for short-crested wave instabilities associated with harmonic resonance, the frequencies reach the zero-axis, remain on that axis within a $\phi_{1,1}$-range and then leave it, yielding

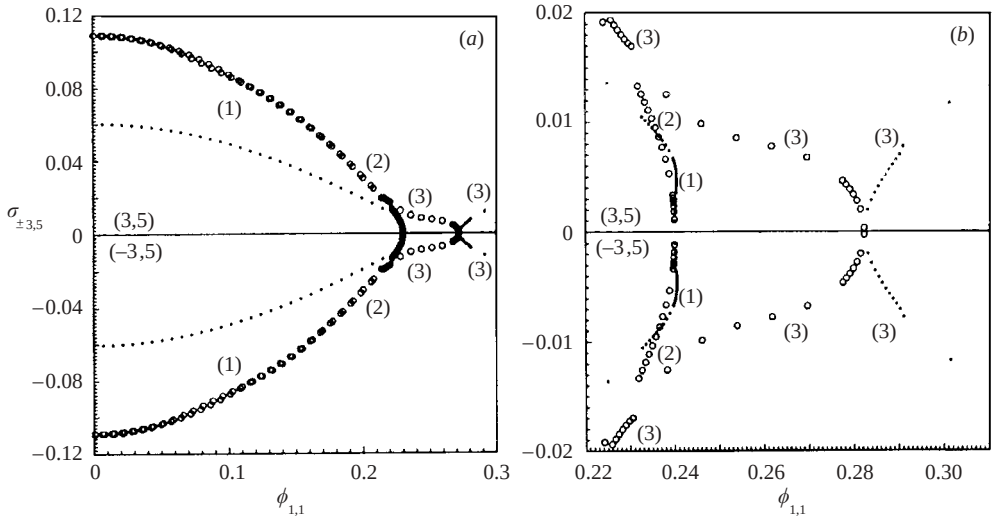

FIGURE 4. Frequency $-\mathrm{Re}(\sigma_{\pm 3,5})$ ($\cdot$) and growth rate $-\mathrm{Im}(\sigma_{\pm 3,5})$ ($\circ$) as a function of $\phi_{1,1}$ for $\theta = 0.001^\circ$ and $d = 0.58$: branches are denoted similarly to those of figure 2. As noted in the figure, positive values of the frequencies and growth rates correspond to $\sigma_{3,5}$ and negative values correspond to $\sigma_{-3,5}$. Since either the frequency or the growth rate vanishes, only the non-zero values are plotted (except at zero where both quantities vanish). Panel (*b*) is an enlargement of (*a*).

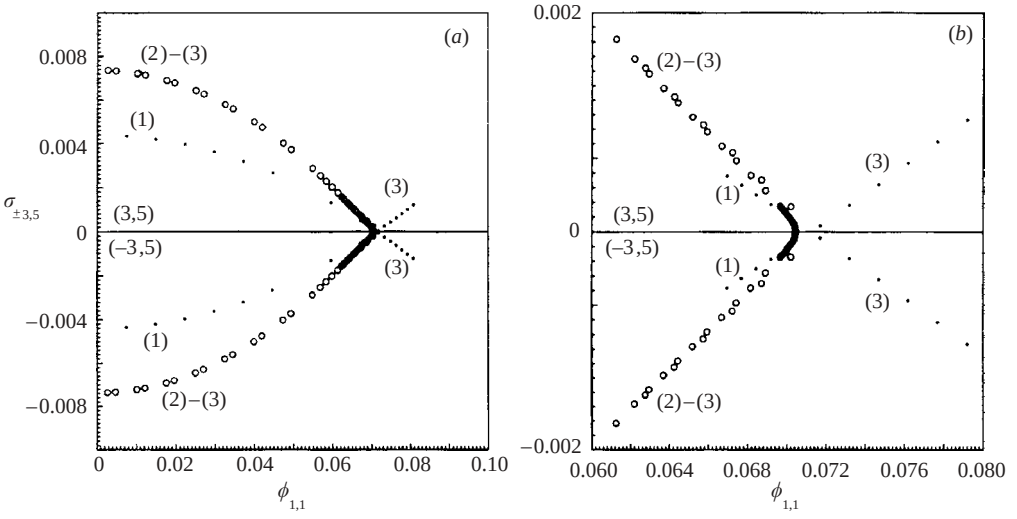

FIGURE 5. Same as figure 4 except for $d = 0.62$.

a 'bubble' structure of the instability. This has been shown in particular by Ioualalen & Okamura (2002) for the harmonic resonance (2, 6) which is characteristic of three-dimensional short-crested waves. In the present case, i.e. for standing waves, the region of instability is located in a wide range of $\phi_{1,1}$, which is quite different. The instability is strong for resonant waves, i.e. on branch (2) and the left-hand part of branch (3) where coefficient $\phi_{3,5}$ is dominant. The instability weakens as $\phi_{1,1}$ increases. Beyond the turning point, branch (3) remains weakly unstable within a certain range of the

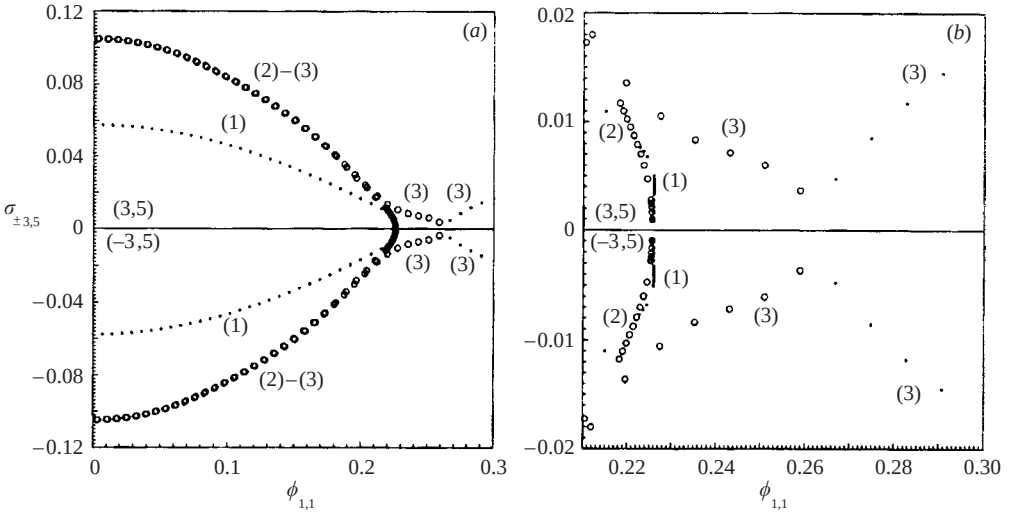

FIGURE 6. Same as figure 4 except for $\theta = 5°$.

parameter regime and then it turns stable. Figure 6 indicates the frequencies and growth rates of the eigenvalues $\sigma_{\pm 3,5}$ for depth $d = 0.58$ and $\theta = 5°$ which is not at the standing wave limit. The results in figure 6 are similar to those in figure 4. The diagrams of this instability are thus characteristic of harmonic resonances due to the standing wave limit of short-crested waves even when the wave is three-dimensional.

To conclude: since we have shown that the solutions of short-crested waves match those of 'pure' standing waves at their limit $\theta \to 0°$, we may apply the above results to two-dimensional standing waves.

5. Conclusion

This study deals with the ability of two-dimensional free-surface standing waves to admit multiple solutions and with the associated existence of harmonic resonances yielding superharmonic instabilities. These resonances are a particular feature of two-dimensional standing waves exhibiting a multiple solution structure. This non-uniqueness is analysed through numerical computation of the waves; we then studied their stability near the region of the parameter regime where the strongest harmonic resonance (3,5) occurs. Since our numerical procedure to compute the stability of three-dimensional short-crested waves does not apply to two-dimensional standing waves (because the waves are no longer stationary), we had first to show that short-crested waves and standing waves match each other at the limit $\theta \to 0°$ in order to extend the stability results to standing waves. Then we performed a superharmonic stability analysis of short-crested waves very near their standing wave limit in order to apply the results derived to 'pure' standing waves. The stability analysis shows that resonant waves are strongly unstable. They are likely to jump from one solution to another, e.g. from branch (2) to (3), and their instability is likely to enhance the amplitude of the jump since the gap between the dominant superharmonic modes (3,5) of the two branches of opposite sign may increase with time. By contrast, non-resonant waves are weakly unstable within a sporadic range of the parameter regime and then turn stable. Therefore they are the only solutions to persist.

The authors would like to acknowledge with thanks Hidekazu Tsuji for his constant computational help. This work has been done thanks to the fellowship for COE foreign researchers given to M. I. by the Research Institute for Applied Mechanics, Kyushu University. The authors wish to express their thanks to Robert Farhi and Michel Israel from the French Embassy at Tokyo for their crucial support in completion of this work. Thanks are due to Christian Colin for his constant support.

REFERENCES

Bridges, T. J., Dias, F. & Menasce, D. 2001 Steady three-dimensional water-wave patterns on finite-depth fluid. *J. Fluid Mech.* **436**, 145–175.

Hsu, J. R. C., Tsuchiya, Y. & Silvester, R. 1979 Third approximation to short-crested waves. *J. Fluid Mech.* **90**, 179–196.

Ioualalen, M., Kharif, C. & Roberts, A. J. 1999 Stability regimes of finite depth short-crested water waves. *J. Phys. Oceanogr.* **29**, 2318–2331.

Ioualalen, M. & Okamura, M. 2002 Structure of the instability associated with harmonic resonance of short-crested waves. *J. Phys. Oceanogr.* **32**, 1331–1337.

Ioualalen, M., Roberts, A. J. & Kharif, C. 1996 On the observability of finite depth short-crested water waves. *J. Fluid Mech.* **322**, 1–19.

MacKay, R. S. & Saffman, P. G. 1986 Stability of water waves. *Proc. R. Soc. Lond.* A **406**, 115–125.

Marchant, T. R. & Roberts, A. J. 1987 Properties of short-crested waves in water of finite depth. *J. Austral. Math. Soc.* B **29**, 103–125.

Mercer, R. G. & Roberts, A. J. 1994 The form of standing waves on finite depth water. *Wave Motion* **19**, 233–244.

Okamura, M. 1996 Notes on short-crested waves in deep water. *J. Phys. Soc. Japan* **65**, 2841–2845.

Roberts, A. J. 1983 Highly nonlinear short-crested water waves. *J. Fluid Mech.* **135**, 301–321.